Using DTI to predict the cortical circuits affected by deep brain stimulation in individual patients.

605.14

B. K. Fahrenthold[1], B. D. Greenberg[2], S. Rasmussan[2], E. Eskandar[3], N. Makris[3], G. M. Papadimitriou[3], D. D. Dougherty[3], J. F. Lehman[1], S.N. Haber[1].

[1]Dept. of Pharmacology and Physiology, University of Rochester School of Medicine & Dentistry, Rochester, NY, USA, [2]. Butler Hospital, Providence RI, [3]. Massachusetts General Hospital, Boston, MA.

INTRODUCTION

Deep brain stimulation (DBS), a therapy being investigated for obsessive-compulsive disorder (OCD) and depression, targets the cortico-basal ganglia circuit by placing the electrodes in the ventral anterior internal capsule (VC) and adjacent ventral striatum (VS) (Greenberg et al., 2010).

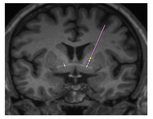

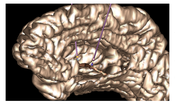

Left: Electrode with contacts superimposed on a patient's MRI. Not all contacts are seen at the same coronal level. Right: 3-D model of electrode placement

The overall goal of this study was to better understand the underlying circuit that is affected during DBS in OCD patients by using probabilistic diffusion tensor imaging (DTI) tractography to evaluate the likely pathways involved at each of the DBS contacts in individual patients.

Several ascending and descending fiber bundles pass through the VC/VS site, each of which may differentially modulate behaviors and, thus, impact OCD-depressive symptoms. Based on nonhuman primate tracing studies, we have shown that in both monkeys and humans, cortical fibers enter and are positioned within the IC according to specific rules, (see posters 605.10 and 605.11). However, although significant advances in DTI tractography have addressed many technical problems, they are not completely resolved. Thus DTI can result in false positives which we address here.

We placed seeds at each electrode contact for each of three patients, B2, B3, & M2 (see below) to determine: 1. The pathways and structures likely to be involved at each contact for each patient; and 2. Which pathways are likely to be accurate and which are likely to be false positives using the rules defined from monkey studies.

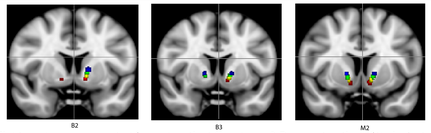

Eight seeds were generated for each patient based on a 3-D reconstruction of their electrode contact locations: red=contact 0, yellow= contact 1, green=contact 2, blue=contact 3)

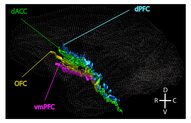

Rules: The position fibers take to enter and travel within the IC depends on the cortical location. Fibers from dorsal PFC regions travel dorsal to those from more ventral areas. Fibers from both more medial and more rostral PFC regions travel ventral to those from more lateral and caudal regions respectively. (See poster 605.10).

FIGURE 1

Several pathways are associated with each contact. Illustrated here are those that are consistent with the expected trajectories based on animal studies. Importantly, the rules that dictate the position of fibers within the IC derived from animal studies are consistent with those seen here. For example, more ventral seeds result in fibers connecting with the vmPFC and through the VAF to the amygdala, while more dorsal seeds result in fibers connecting to more dorsal PFC areas. Note: terminating areas are assumed as DTI shows only the stem of the bundle, not origin or terminal regions.

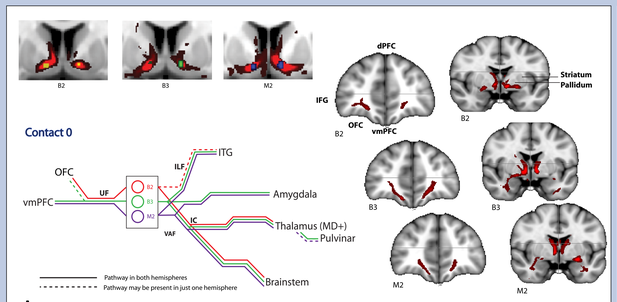

A Probabilistic pathways generated using contact 0 as the seed. In all patients pathways are connected to the region of the vmPFC/OFC via the UF. Caudally, pathways travel through the ILF connecting the ITG. In addition, pathways in patients B3 and M2 pass through the VAF connecting with the amygdala. Pathways also connect to the thalamus including medial dorsal n. and the pulvinar, and to the brainstem.

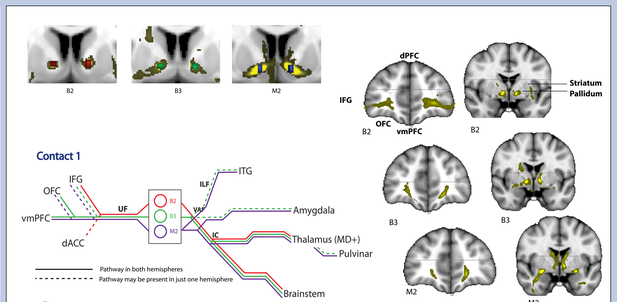

B Probabilistic pathways generated using contact 1 as the seed. B3 and M2, but not B2, pathways continue to connect with the vmPFC/OFC via UF, through the ILF with the ITG, and through the VAF with the amygdala. B2 pathways (whose contact is dorsal) travel dorsal and lateral through the WM connecting with the IFG. Fibers from contact 1 in B2 do not travel through the ILF or the VAF. Fibers from all contact 1 seeds connect with the thalamus and brainstem.

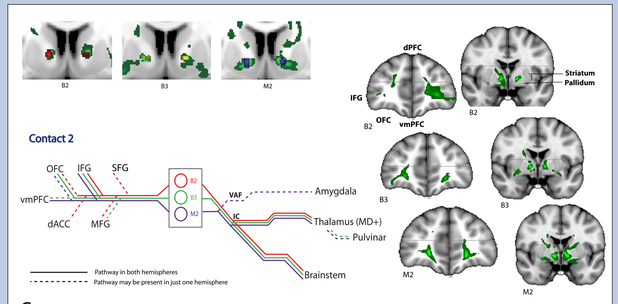

C Probabilistic pathways generated using contact 2 as the seed. Fewer bundles from this more dorsal contact connect with the vmPFC. Caudally, B3 and M2 pathways could not be followed through the ILF to/from the ITG or through the VAF. B2 and B3 pathways connect with the MFG. In addition, B3 pathways connect with more dorsal PFC regions, the SFG and dACC. Fibers continue to connect with the thalamus and brainstem.

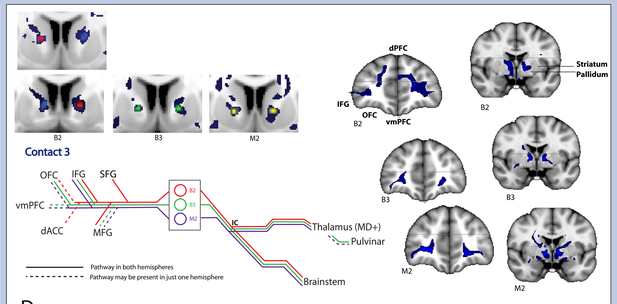

D Probabilistic pathways generated using contact 3 as the seed. Pathways of all three patients connect with the IFG. Pathways in B3 and M2 continue to the vmPFC/OFC. In contrast, B2 fibers connect to the SFG and dACC. As with the other contacts, fibers traveled to/from the thalamus and brainstem.

FIGURE 3

DTI tractography results from patient B3.

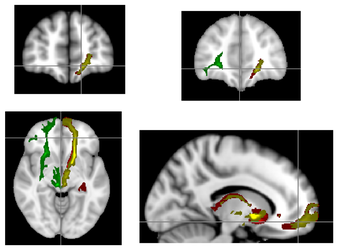

A Coronal, horizontal, and sagittal sections from patient B3 illustrates the pathways from the active contacts (L0, L1, R2). Pathways move rostrally toward the vmPFC and vlPFC via the UF and caudally in the IC to/from the thalamus, continuing to the pulvinar.

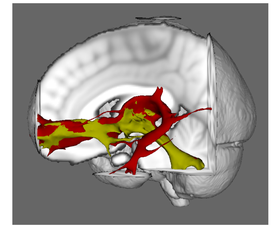

B Sagittal view of 3-D probabilistic tractography of contacts L0 and L1 in B3. The dorsal-ventral relationship of the pathways generated is visible, with the most ventral contact showing a pathway tracking ventrally in the PFC and the most dorsal contact tracking to/from more dorsal PFC.

RESULTS & CONCLUSIONS

1. Several pathways are associated with each contact. Note: terminating areas are assumed, as DTI shows only the stem of the bundle, not origin or terminal regions.

2. Contacts for each patient are positioned somewhat differently. Contacts for B2 are most dorsal and those for M2 are most ventral. These differences are within the typical individual variation. However, interestingly, the ventral/dorsal seed positions are reflected in different pathway trajectories.

3. Many pathways are consistent with the expected trajectories based on animal studies. Importantly, the rules that dictate the position of fibers within the IC derived from animal studies are consistent with those seen here (see Posters 605.10, 605.11 and 605.12). For example, more ventral seeds result in fibers traveling to vmPFC and through the VAF to the amygdala, while more dorsal seeds result in fibers traveling to more dorsal PFC areas (see Fig. 1).

4. Several pathways associated with each contact were not consistent with the expected trajectories based on animal studies (false positives) (Fig. 2). We determined a pathway to be a false positive using 2 criteria. First, it did not follow rules derived from the monkey tracing studies. Second, we could find a likely alternative route, but not a direct one. The alternative route required at least 1 'jump' into another WM bundle.

5. While all seeds show connections with the brainstem, the connection details varied considerably across contacts.

6. Patient B3 had the greatest therapeutic response, based on the YBOCS score. The active electrodes were Left (L) 0-, 1-, C+ and Right (R) 2-, C+. The active electrodes in both patients B2 and M2 were more dorsal (B2; L2-, 3-, C+; R off: M2; L2-, C+; R1-, 2-, C+) (Fig. 3).
**The electrical field generated at each contact will encompass a larger area than illustrated here.

Summary:
Consistent with monkey tracing data, DTI tractography demonstrates that the connections associated with each contact can be traced to specific prefrontal cortical areas. However, many false positives connections were found. Taken together, the interpretation of DTI results depends on a clear prior understanding of how structures are connected using experimental animal data.

Preliminary results suggest that activation of ventral prefrontal cortical connections, including the vmPFC, OFC, and IFG, may be key for effective therapy. All contacts included connections to the thalamus and brainstem. However, specific thalamic brainstem regions associated with each contact remain to be determined.

METHODS

Three patients receiving DBS for treatment resistant OCD were included in this study. Patient B2's primary symptom was incompleteness. After 12 months of DBS therapy, the YBOCS score showed a 23% reduction. Patient B3's primary symptoms were incompleteness and harm avoidance. After 12 months of therapy, the YBOCS score showed a 23.3% reduction. Patient M2's primary symptom was harm avoidance. After 12 months of therapy, the YBOCS score showed a 53% reduction.

Preoperative MRIs and DTIs (3T Siemens scanner) and a postoperative CT scan were obtained for each patient. The number of angles = 60. Preoperative MRIs and postoperative CT scans were merged to identify the exact electrode placement. A 3-D reconstruction of the electrode placement and contact position was made. All of the MRI data analyses were done using tools from FSL 4.1.9 (Smith et al., 2004, Woolrich et al., 2009). The data was corrected for field inhomogeneity-induced distortions prior to averaging (Andersson et al., 2003). The quality of this preprocessing step was visually checked using FLIRT rigid-body registration (Jenkinson et al., 2002) to the subjects' distortion-free T1-weighted structural images. Probabilistic pathways were generated for each contact for each patient in FSL using seed masks with dimensions of the electrode contacts registered in MRI space. A midline exclusion mask was used to limit tracts from crossing the corpus callosum. Data from each patient were than transformed into standard MNI152 space to make direct comparisons between patients. Data registered to standard MNI152 space (1mm isotropic) used a two-stage registration: (1) rigid-body alignment of a fractional anisotropy (FA) image to the T1-weighted structural of each individual, then (2) nonlinear (FNIRT) transformation to standard space using a high resolution distortion model. Pathways were compared to the expected trajectories from animal experiments to identify those pathways likely to be correct from those likely to be false positives.

FIGURE 2

Several pathways associated with each contact were not consistent with the expected trajectories based on animal studies (false positives).

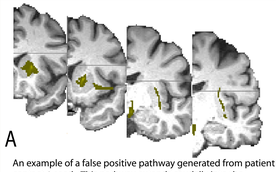

A An example of a false positive pathway generated from patient B2, contact 1 seed. This pathway extends caudally into the external/extreme capsules (EC/EmC). However, tracing experiments show that fibers traveling in the external and extreme capsules enter them as they leave the cortex, they do not pass through the IC (see B). However, ventral PFC fibers split as they leave cortex, with one branch entering the IC, and the other entering the EC/EmC. Thus, the likely explanation for how DTI tracked pathways here, is by following the streamline rostral to the region where fibers enter the 2 capsules, then 'jump' to the external/extreme capsule, 'hitching a ride' caudally.

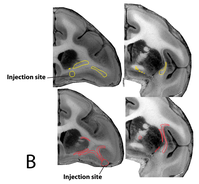

B Animal data demonstrates how fibers traveling from vPFC enter the IC and EC/EmC. Top panel: Fibers leave the cOFC travel dorsally and split into 2 bundles, 1 enters the IC, and 1 turns laterally into the EC/EmC. Bottom panel: Fibers leave the lOCF and travel dorsally and split into 3 bundles, 1 to the UF, 1 to the IC and 1 to the EC/EmC

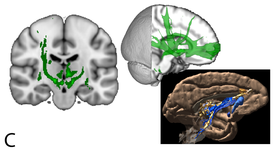

C A pathway generated from patient M2, contact 2 seed, tracts to/from motor areas (top figures). However, motor fibers do not pass through the anterior ventral IC region. They travel in the posterior limb of the IC. Bottom-right figure illustrates the PFC pathway from monkey tracing data. One likely path to motor areas is DTI tracking dorsally, through the striatum and IC, 'jumping' into the subcallosal fasciculus and 'hitching a ride' caudally to hook up with the descending cortico-spinal pathway. Alternatively, the thalamus could provide the link.

REFERENCES

Andersson, J. L., et.al, J. 2003. Neuroimage, 20, 870-88.
Greenberg, B. D., et al. 2010. Molecular psychiatry, 15(1), 64-79.
Jenkinson, M., et. al S. 2002. Neuroimage, 17, 825-841.
Smith, S. M., et. al 2004. Neuroimage, 23 Suppl 1, S208-19.
Woolrich, M. W., et. al. 2009. . Neuroimage, 45, S173-86.

This research supported by NIMH grant MH86400

ABBREVIATIONS:

dACC-dorsal anterior cingulate cortex
dPFC-dorsal prefrontal cortex
cOFC-orbital frontal cortex
EC/EMC-external capsule/extreme capsule
IC-internal capsule
IFG-inferior frontal gyrus
ILF-inferior longitudinal fasciculus
ITG-inferior temporal gyrus
lOFC-lateral orbital frontal cortex
MD-medial dorsal nucleus of the thalamus
lOFC-orbital frontal cortex
MFG-middle frontal gyrus
OFC orbital frontal cortex
SFG-superior frontal gyrus
UF-uncinate fasciculus
VAF-ventral amygdalofugal pathway
vLPFC-ventral lateral prefrontal cortex
vmPFC-ventral medial prefrontal cortex
WM-white matter
YBOCS-Yale Brown obsessive-